GEOSCIENCES REVIEW

GeoRev is a free access journal of Bayero University, Kano, Nigeria https://georev.org/index.php/georev

# Sedimentology and geochemistry of Bima Sandstones around Hinna, Gongola Basin, Northern Benue Trough: Implications for paleoenvironment, provenance, tectonic setting, and paleo-weathering

Ahmad Umar Ibrahim Bebi*[1], Sani Kasim[2]
Department of Geology, Bayero University, PMB 3011, Kano State, Nigeria

ARTICLE INFORMATION

PISSN 3141-3021 EISSN 3141-303X

**Article history:**
Received 1 February 2026
Revised 7 May 2026
Accepted 19 June 2026
Available online 29 July 2026

**Keywords:**
Bima sandstone
Paleoweathering
Provenance
Sedimentology
Minerals

https://doi.org/10.70882/georev2026.2(1)14

ABSTRACT

The Bima Sandstone represents the earliest continental infill of the Gongola Basin within the Northern Benue Trough, formed during Early Cretaceous intracontinental rifting associated with the opening of the South Atlantic. This study integrates sedimentological logging, petrography, heavy-mineral analysis, and major–trace-element geochemistry to reconstruct the depositional environment, provenance, tectonic setting, and paleoweathering history of the Bima Sandstone exposed around Hinna. Facies analysis identifies three genetically related facies associations—proximal braided river, braided river in-channel, and floodplain/overbank—indicating deposition in a high-energy braided fluvial system with upward transition to lower-energy overbank settings. Petrographic results classify the sandstones as arkosic to lithic arkosic, dominated by quartz and feldspar with subordinate lithic fragments, reflecting short transport distances and rapid sediment supply. Heavy mineral assemblages are characterized by zircon, rutile, and tourmaline with moderate ZTR indices, supporting derivation from felsic igneous and high-grade metamorphic basement sources. Geochemical signatures, including high $SiO_2$ contents, felsic-dominated trace-element ratios, and elevated CIA, CIW, and PIA values, indicate moderate to intense chemical weathering of granitic and gneissic source rocks. Tectonic discrimination diagrams consistently place the sandstones within the continental rift field, confirming syn-rift sedimentation controlled by fault-related subsidence and basement uplift. Collectively, the Bima Sandstone at Hinna records a multi-cycle, syn-rift braided fluvial succession deposited in a fault-controlled intracontinental rift basin, refining the tectono-sedimentary evolution of the Gongola Basin and contributing to improved basin analysis and reservoir characterization in the Upper Benue Trough.

Peer review under the responsibility of Bayero University, Kano. ©
Corresponding author. E-mail address: ahmadbebi01@gmail.com (Ahmad, U.I. B. and Sani K.)



## INTRODUCTION

The detrital components of siliciclastic rocks, particularly sandstones, provide vital insight into understanding the evolution of the Earth's crust, as they preserve crucial records of provenance, tectonic setting, paleoclimate, and depositional environments. Sandstones, composed of sand-sized particles, are directly influenced by weathering, transportation, deposition, and diagenesis, which collectively determine their mineralogical and geochemical signatures (Cox et al., 1995; Pettijohn et al., 1987). Sedimentological studies have gained increasing importance as the discovery of new sedimentary deposits becomes progressively more challenging. The mineralogy and chemistry of sandstones are strongly tied to the nature of their parent rocks and the tectonic regimes in which they formed. Consequently, systematic investigations of sandstone composition have long been recognized as essential for unraveling crustal evolution and for assessing their reservoir quality in hydrocarbon exploration (Critelli et al., 2003; Dickinson & Suczek, 1979).

Petrographic analysis provides a robust framework for sandstone classification and provenance interpretation by identifying framework grains and textural attributes (Dickinson et al., 1983). Complementarily, major-element geochemistry offers quantitative constraints on source rock composition, chemical weathering intensity, sediment recycling, and tectonic regime (Bhatia, 1986; Roser & Korsch, 1986; Nesbitt & Young, 1982). Heavy-mineral assemblages further refine provenance interpretations because they are resistant to mechanical and chemical alteration, thereby preserving diagnostic source signatures (Hubert, 1962; Mange & Wright, 2007). These integrated methods are especially relevant to the Benue Trough, a major intracontinental rift basin within the West and Central African Rift System that developed during the Early Cretaceous in response to regional extensional tectonics associated with the opening of the South Atlantic (Genik, 1993; Benkhelil, 1989). The Gongola Sub-basin represents a structurally controlled segment of this rift system, where normal faulting and basement uplift strongly influenced sediment supply and the development of accommodation (Zaborski et al., 1997; Abubakar, 2006).

The Bima Sandstone, which unconformably overlies the Precambrian Basement Complex, constitutes the oldest sedimentary unit in the Gongola Basin and is dominated by fluvial deposits ranging from conglomerates to sandstones and mudstones (Falconer, 1911). Despite extensive regional studies, detailed integrated petrographic, heavy-mineral, and geochemical constraints on the Bima Sandstone exposed around Hinna remain limited. This study, therefore, applies a multi-proxy approach to elucidate the sedimentary facies of the Early Cretaceous continental sediments of the Bima Formation (Middle Bima Member) exposed around Hinna, Gongola Basin, to unravel their provenance, paleoenvironment, and paleoweathering using lithofacies analysis, mineralogy, and geochemistry.

The area is distinguished by flat terrain with sandstone hills. Scattered shrubs and thorn bushes are typical vegetation types in the area. The area is accessible via a network of footpaths, with a single major road passing through.

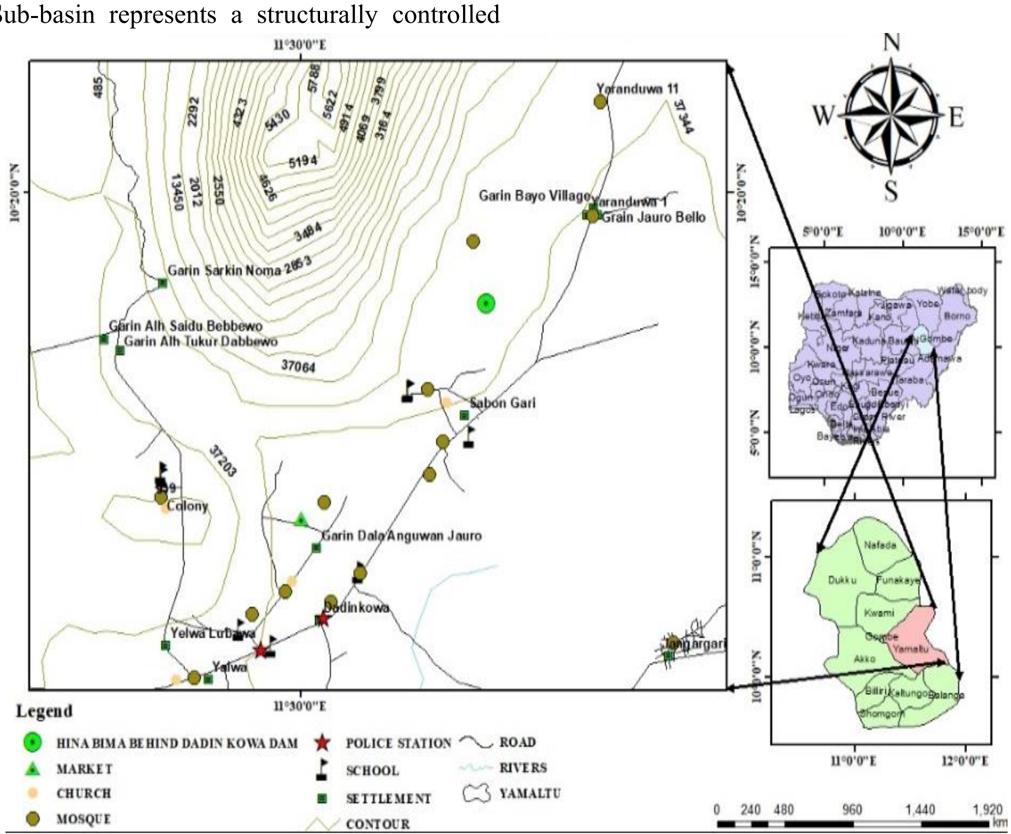


Fig. 1: Map of the study area

*Geology and Stratigraphic Settings*

The Northern Benue Trough forms part of the West and Central African Rift System, developed during the Early Cretaceous in response to the separation of the African and South American plates. It is an elongated intracratonic rift basin trending NE–SW, extending for over 1,000 km and attaining sedimentary thicknesses of more than 6,000 m (Abubakar, 2014; Sarki Yandoka et al., 2014). The origin of the trough has been linked to both rift-related extensional tectonics (King, 1950; Genik, 1993) and wrench-faulting models involving transcurrent strike-slip motion (Benkhelil, 1986; Guiraud & Maurin, 1992). Regardless of these contrasting models, its structural architecture is characterized by horst-and-graben systems, controlled by deep-seated faults that influenced subsidence and sedimentation patterns (Benkhelil et al., 1989; Abubakar, 2006). Structural highs such as the Dumbulwa-Bage Ridge divide the Northern Benue Trough into the Yola Basin, which trends E-W, and the Gongola Basin, which trends N-S (Zaborski, 1998). The Nigerian Basement Complex surrounds the Gongola Basin to the west and the Adamawa Massif to the east. At the same time, sinistral strike-slip faults such as the Gombe, Bima-Teli, and Kaltungo faults exerted significant tectonic control during their evolution (Maurin et al., 1986).

The Northern Benue Trough's geologic succession records syn- and post-rift sedimentation. The oldest unit is the continental Bima of Late Jurassic to Albian age, which lies unconformably on the Precambrian Basement Complex (Fig. 2), comprising conglomerates, coarse- to fine-grained sandstones, and mudstones deposited in alluvial-fan and braided-fluvial systems (Guiraud, 1990; Zaborski et al., 1997). This is overlain by the transitional Yolde Formation of Cenomanian age, which lies conformably on the Bima Sandstone, reflecting a shift from continental to shallow-marine environments. Above this, the Pindiga Formation records a major marine transgression during the Cenomanian–Turonian, dominated by shale-limestone successions. The Yolde Formation in the Gongola Arm is conformably covered by the laterally equivalent Gongila and Pindiga Formations. These formations, which are lithologically defined by pale and dark carbonaceous limestones and shales with minor sandstones, represent a complete marine incursion into the Upper Benue during the Turonian-Santonian periods. The Turonian-Santonian counterparts of the Gongila and Pindiga Formations in the Yola Arm are the Dukul, Jessu, Sekule, and Numanha Formations. The Campanian–Maastrichtian Gombe Formation in the Gongola Basin and the Lamja Sandstone in the Yola Basin, both distinguished by fluvio-deltaic deposits, lie above these successions. The Tertiary Kerri-Kerri Formation caps the sequence, representing a continental deposit of sandstones and siltstones with abundant coal intercalation (Abubakar, 2014; Nwajide, 2013).

## MATERIALS AND METHODS

This study employed a combination of fieldwork and laboratory analyses (petrographic, heavy-mineral, and geochemical analyses).

*Field work and sampling*

Grain size, texture, bedding features, lithology, and sedimentary structures were key parameters recorded during fieldwork to enable detailed stratigraphic logging of exposed sections and to understand the observed structures and textures. Overall, this offers guidance on how to approach the section. Fresh representative samples were taken at stratigraphic intervals and recorded for laboratory analysis. Measurements of bed thickness, coordinates, sedimentary features, and lithological characteristics of the rock were also systematically recorded.

***Petrographic analysis***

Petrographic investigations were conducted on thin sections prepared from ten different samples. These thin sections were prepared at the thin sections laboratory, Department of Geology, University of Maiduguri, and studied using standard polarizing microscope coupled with a digital camera at Department of Geology, Bayero University Kano for minerals identification under both plane polarized light (PPL) and cross polarized light (XPL), in order to identify framework grains like quartz, feldspar, lithic fragments, and accessory minerals. Modal examination employed the Gazzi-Dickinson point-counting method for sandstone classification and provenance interpretation. The petrographic data were presented in a standard ternary QFL diagram.

*Heavy mineral analysis*

Five chosen samples were air-dried, crushed, and pulverized to a sieve size. 15 g of each sample was washed and boiled with HCl for 10 min to remove any possible iron coating and cementing materials. Bromoform was used to separate the heavy minerals. Samples of the heavy fraction were then cleaned with acetone on filter paper, dried in an oven set at 80 degrees, weighed, and finally placed on a glass slide. A binocular petrological microscope was used to quantitatively estimate the heavy minerals present in the samples.

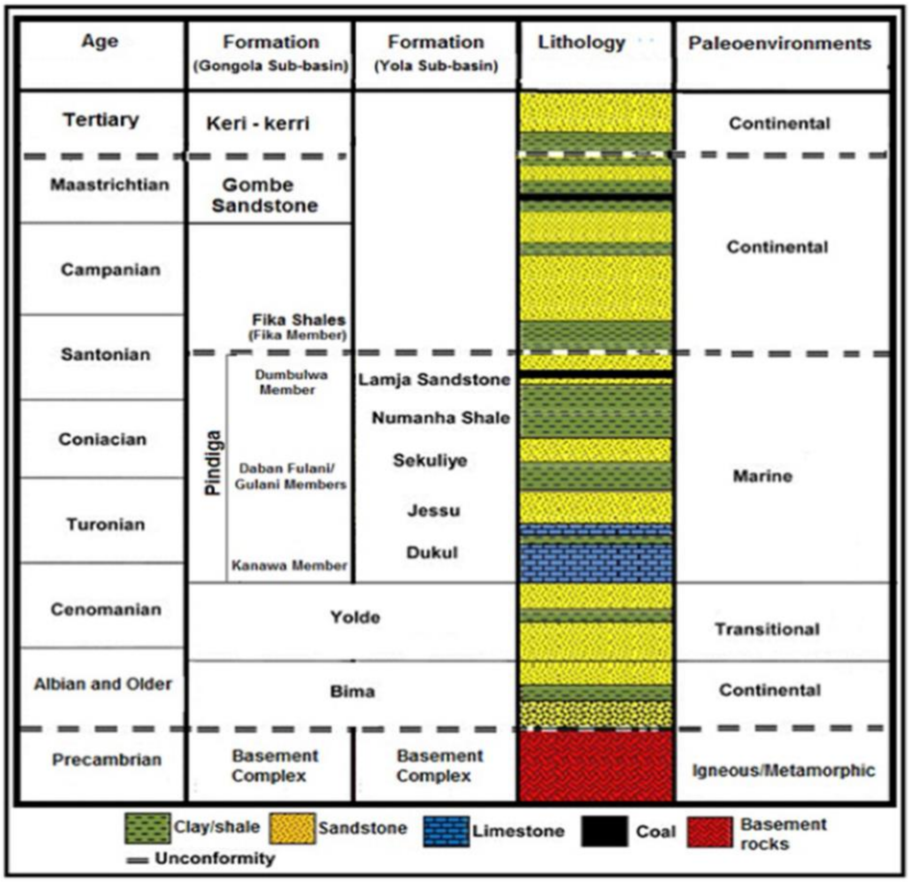

**Fig. 2:** Stratigraphic succession of Gongola Basin showing the position of Bima Sandstone (after Sarki Yandoka 2015)

*Geochemical analysis*

The major element composition was ascertained using X-ray fluorescence (XRF) analysis. To facilitate easy pulverization with a Retsch PM 400 planetary ball mill, the samples were first dried in an oven to remove any remaining moisture. While the powdered samples were bagged and labeled for analysis, the ground samples were ensured to pass the 150-micron sieves. The examination was conducted using an Energy-Dispersive X-ray Fluorescence (EDXRF) spectrometer of the "Epsilon 4" model, manufactured by PanAlytical in the Netherlands. One gram of the powdered sample was heated to 1000 degrees Celsius. In a weighed and cleaned crucible to determine the loss-on-ignition (LOI) by gravimetry. The crucible and its contents were then weighed to determine the weight difference before and after heating. Each prepared sample, weighing 20g, was placed in a sample cup. On the sample changer, the cups containing the contents were properly positioned in their appropriate measuring positions. Overall, after the LOI procedure and the values are obtained, they are entered into the machine for each sample, and the analysis is conducted. The chemical composition of each sample is obtained by adding the LOI to its concentration.

## RESULTS AND DISCUSSIONS

*Lithostratigraphy and facies analysis*

The outcrops of the Middle Bima Member around the Hinna of the Gongola Basin are characterized by very coarse to fine-grained, thick-bedded sandstones interbedded with mudstones and conglomeratic horizons containing cobbles and pebbles of mainly rock fragments (gneissose, granitic, volcanic, and occasionally sedimentary), quartz, and feldspar. The sandstones are predominantly white to grey, occasionally brown, and range in grain size from fine to very coarse. Coarse to pebbly facies commonly exhibit trough and planar crossbedding, erosional bases, and mudclast lags, consistent with deposition in high-energy fluvial systems. Mudstones are typically dark grey to brownish-grey, friable, and occur as thin beds.

A total of 80.5 meters of thickness was logged overall (Fig. 3), comprising nineteen fining-upward cycles. Each cycle begins with coarse-grained, erosionally based sandstones that grade into finer sandstone or mudstone units, reflecting repeated channel deposition followed by waning flow conditions. The section's lower portion is dominated by poorly sorted, pebbly, very coarse-grained sandstones with cross-bedding and erosional mud clasts. At the same time, the middle interval consists mainly of medium- to coarse-grained friable sandstones with clay partings. The upper portion is capped by mudstones interbedded with fine sandstones, reflecting a reduction in depositional energy upward through the sequence.

Facies analysis of the Middle Bima Member (Bima II) exposed around Hinna in the Gongola Sub-basin was carried out following the lithofacies scheme of Miall (1977, 1978, 1996, 2010). Eight lithofacies were identified which includes: Gravelly bedded sandstones (Gtt), Pebbly-coarse grain sandstone (Gtb), trough cross bedded sandstones (St), massive sandstones (Sm), tabular (planar) cross bedded sandstones (Sp), Silts and sand (Fm), Mud and sand (F12) and mudstones (F11) facies based on lithology, grain size, sedimentary structures, bounding surfaces, and vertical stacking patterns. The succession is characterized by repeated fining-upward cycles, erosional basal contacts, and an upward decrease in depositional energy, reflecting deposition within an evolving syn-rift fluvial system of the Northern Benue Trough. The facies code adopted herein was based on the scheme of Miall (1978, 1996, 2010)

***Gravelly bedded sandstone facies (Gtt)***

The Gtt facies comprises very coarse- to coarse-grained sand with angular to sub-rounded grains, gravelly sandstones containing abundant pebble- to cobble-sized clasts of gneiss, granite, volcanic rocks, minor sedimentary lithologies, quartz, and feldspar (Fig. 4a). Beds are thick (1–5 m), poorly sorted, and commonly display large-scale trough cross-bedding, erosional bases, and mud clast lags. These facies are interpreted as deposition from high-energy traction currents within deeply incised channels of a proximal braided river system. The erosional bases and mud clast lags reflect repeated channel incision during peak discharge events, typical of syn-rift tectonic settings where high gradients and rapid sediment supply prevail (Miall, 1978; Guiraud, 1990; Abubakar, 2006).

*Through cross-bedded sandstone facies (St)*

Medium- to coarse-grained sandstones arranged in well-developed trough cross-beds (fig. 4f-e) with bed thickness of 1.5 to 6 m. The sandstones are friable and commonly show sharp or erosional lower contacts. The St facies reflects migration of three-dimensional dunes within active braided river channels. It records moderate- to high-energy flow conditions and sustained bedload transport, typical of channel belts in syn-rift fluvial basins (Miall, 1977, 2010).

*Planar cross-bedded sandstone facies (Sp)*

Fine- to medium-grained sandstones with well-developed tabular cross-bedding (fig. 5a-b) with buff colored. Individual sets range from 0.4 to 1.2 m thick and are laterally extensive. Sp facies represents deposition by two-dimensional dunes and transverse bars under relatively stable flow regimes. It is characteristic of mid-channel bar complexes within braided rivers (Miall, 1996)

*Massive sandstone facies (Sm)*

Sm facies are composed of structureless, medium- to coarse-grained sandstones (Fig. 5c) that are 0.7–1.5 m thick and lack internal stratification. These facies are interpreted as rapid deposition from high-concentration flows, possibly during channel infill or sheet floods. Such deposits are common in braided river systems affected by episodic high-magnitude floods and rapid sedimentation linked to tectonic activity (Nichols, 2009)

*Silt and fine sand facies (Fm)*

Laminated siltstone and very fine sandstone units, approximately 2 m thick, with sand bodies that appear to be thicker, commonly occur as interbeds within coarser facies. This facies records low-energy suspension settling during waning flood stages or channel abandonment, representing overbank or distal channel environments (Miall, 1977; Nichols, 2009)

*Pebbly–coarse-grained sandstone facies (Gtb)*

Consists of coarse to very coarse-grained sandstones with scattered pebbles up to 7mm (fig.4b & c), with bed thicknesses of 1–3 m, and moderate to poor sorting. Sedimentary structures include planar and trough cross-bedding, erosional scours, and pebble lags (fig. 4d). This facies represents longitudinal and transverse bar deposits within active braided channels. The abundance of coarse material and cross-bedding indicates strong unidirectional flow, and the pebbly nature and poor sorting suggest rapid deposition near sediment sources, consistent with braided river systems that developed during active rifting in the Benue Trough (Miall, 1996; Zaborski et al., 1997).

*Interbedded mudstone and sandstone facies (F12)*

Alternating beds of mudstone and fine sandstone form thick successions (up to 12 m). Mudstones are laminated, dark grey to brownish-grey, and friable (fig. 5d). F12 reflects episodic floodplain sedimentation, including crevasse splay deposits and overbank flooding. The alternation of sand and mud indicates fluctuating discharge conditions within a broad floodplain setting.

*Mudstone facies (F11)*

Thin (0.2–1 m), dark grey to brownish-grey mudstone beds (Fig. 5e) with poor consolidation and minimal internal structures. This facies represents quiet-water deposition on distal floodplains or in abandoned channels, where fine sediments settled from suspension under very low- energy conditions.

*Sandstone petrography*

Observed detrital components of the sandstones include quartz, feldspars, lithic fragments, matrix (clays and detrital silts), and accessory minerals (Fig. 6). The grains are very coarse to fine grained, subangular to rounded in shape, and are poorly to well sorted. Different grain contacts were observed, including float, point, and long, with predominance of point contact. The Folk method was used to categorize the sandstone (Fig. 7). The quantity of quartz, feldspar, and lithic fragments ranges from 38-66%, 24-52%, and 8-12%, respectively (Table 1)
.

*Quartz*

With an average of 59%, quartz is the most prevalent framework grain in sandstone samples. Typically, quartz grains are subangular to subrounded. Inclusions of tourmaline, zircon, and rutile are often found in some quartz grains. Common contact types include long and point contact. There are both monocrystalline (Qm) and polycrystalline (Qp) quartz grain varieties; monocrystalline quartz grains account for up to 90% of the total quartz grains.

*Feldspar*

The feldspar minerals found are plagioclase feldspar, with alkali feldspar predominating. The microcline and plagioclase feldspars are subordinate to the orthoclase. The majority of the grains range from sub-angular to sub-rounded. Feldspar grains account for an average of 32.5% of total grains in the samples, with a range of 24-52%. Some of the feldspar grains have undergone diagenetic change to sericite. Some are found to have occasionally changed into muscovite or kaolinite, or to have been replaced by calcite. The two most common feldspar minerals, both twinned and untwinned, are albite and orthoclase. While some plagioclases appear to be untwinned, over 80% exhibit twinning.

*Lithic fragments*

The recognized rock pieces, which make up less than 9% of the total grains, are metamorphic, sedimentary, and igneous. The lithic fragments are typically sub-rounded. Muscovite and biotite are the micas in the sandstones, with biotite occurring more frequently than muscovite. The framework grains are bound together by both cement and matrix. Silica, calcite, and clays are the cementing elements that occur as pore fillers.

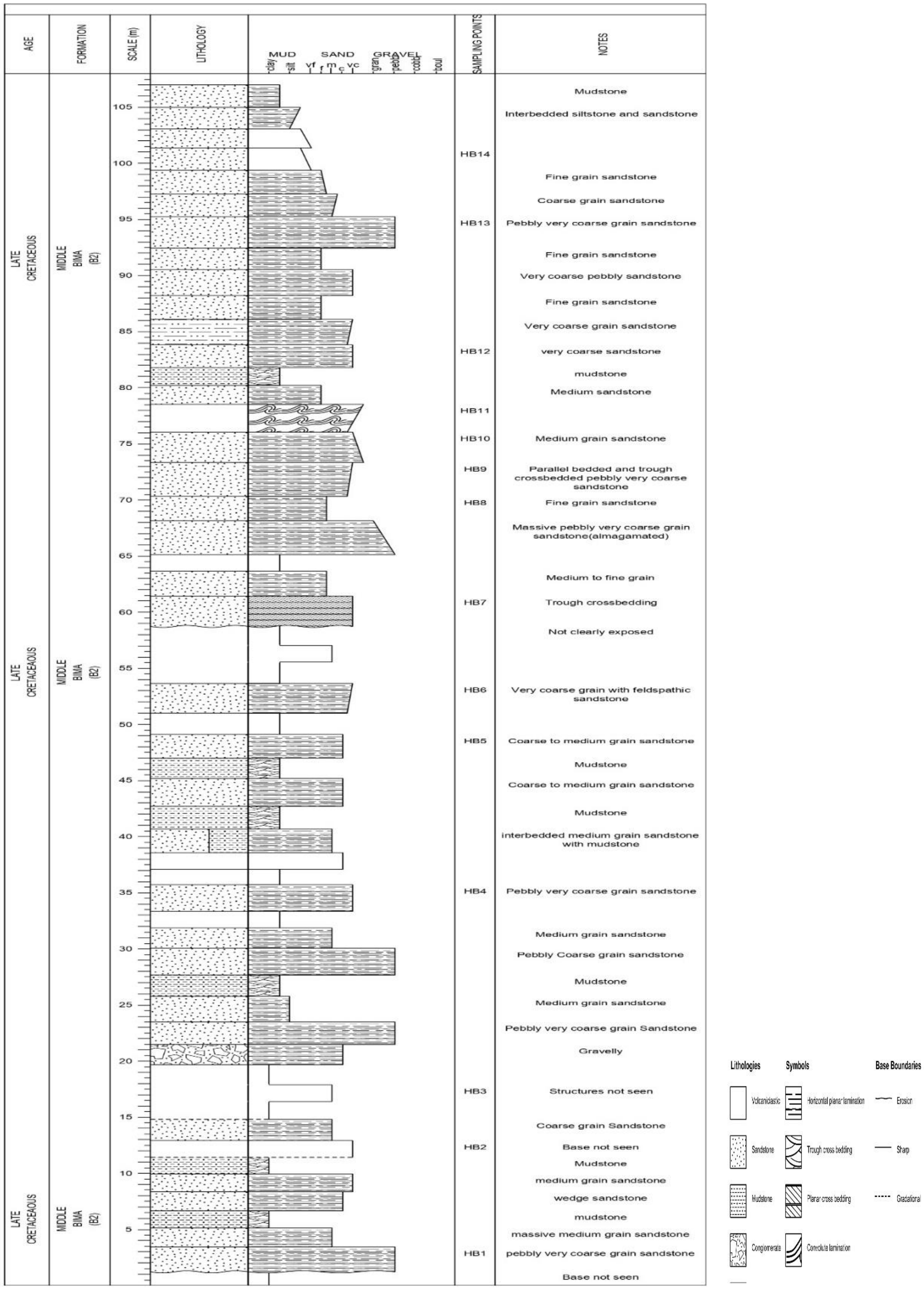


**Fig. 3:** Sedimentary log of the studied section of Bima Sandstone at Hinna Village

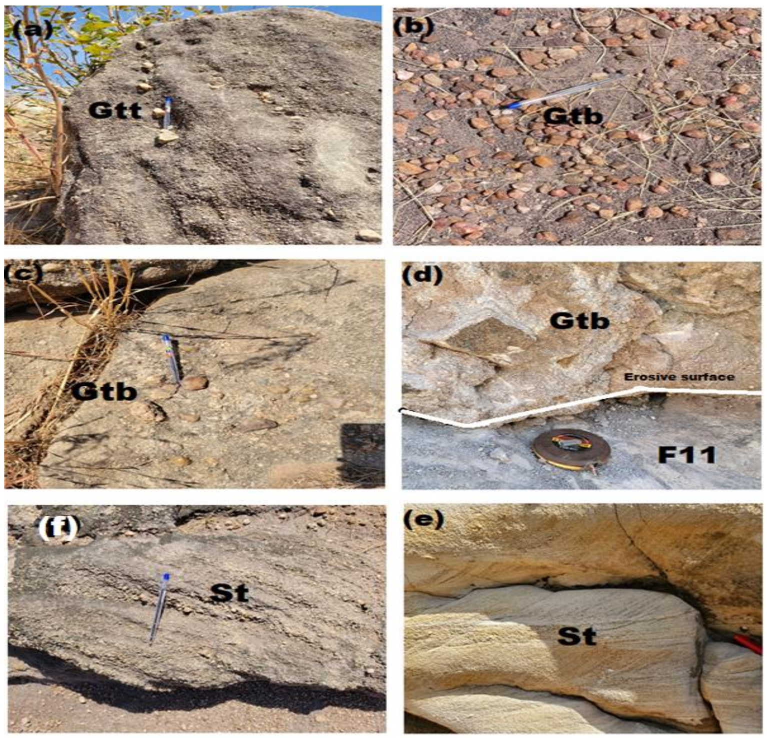


**Fig. 4:** Field photograph (a) Gravelly bedded sandstone facies (b-c) pebbly coarse-grained sandstone facies (d) Erosional contact at the base of pebbly coarse-grained sandstone facies (e-f) Trough cross-bedded sandstone facies

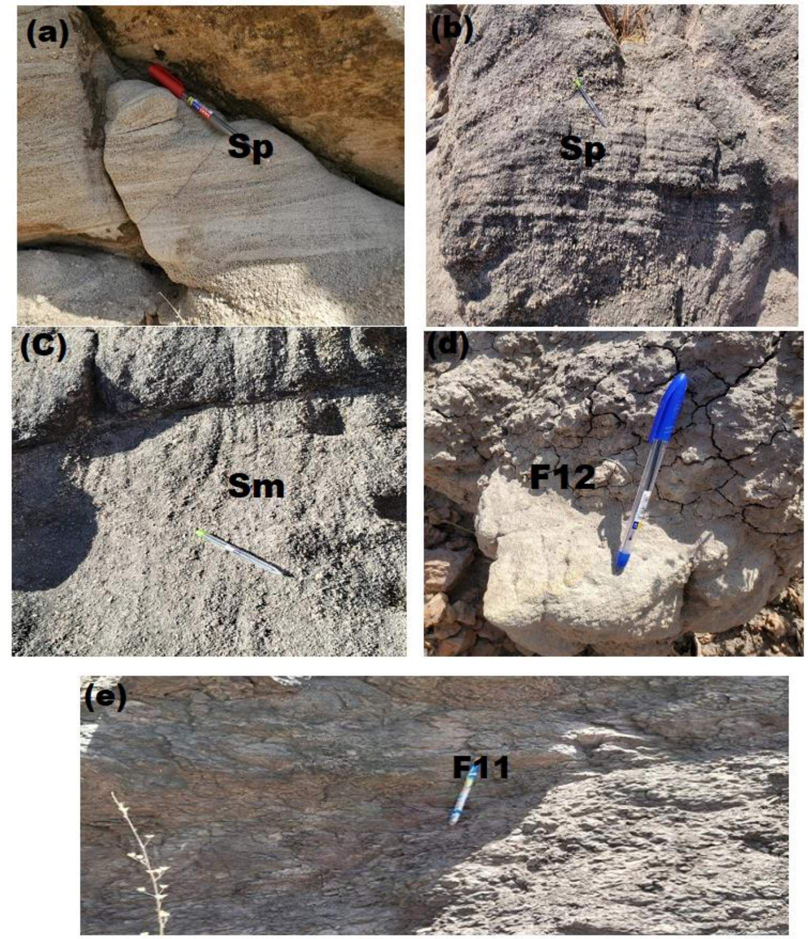


**Fig. 5:** Field photograph (a-b) Planar cross-bedded sandstone facies (c) Massive sandstone facies (d) Mud and Sand facies. (e) Mudstone facies

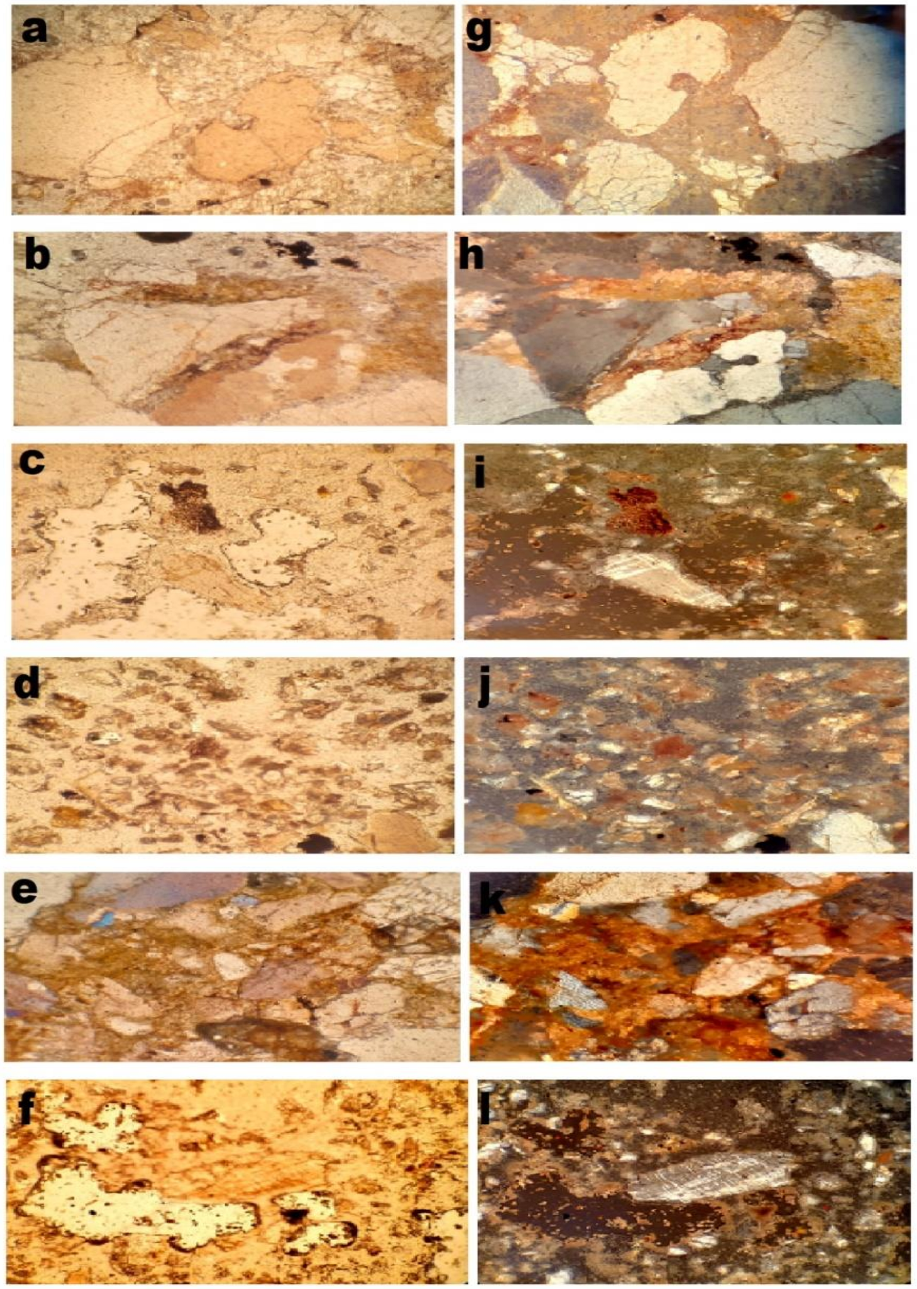


**Fig. 6: Photomicrograph of sandstones** under (a - f) plane polarized light (PPL) and (g - l) crossed polarized light (XPL), Mag. =X40

Based on the method, most samples from the QFL ternary diagram (Fig. 7) are arkosic sandstones, with abundant feldspar and quartz. Some of the samples fall within the Lithic arkose field (HB5, HB11, partially HB2 & HB4), which implies input from orogenic or arc-related sources with a higher proportion of lithic fragments. The absence of Quartz arenite indicates low sediment maturity, supporting short transport distances and/or active tectonics.

*Heavy mineral petrography*

The opaque minerals (such as magnetite, ilmenite, apatite, and garnet), zircon, rutile, and tourmaline comprise the heavy mineral assemblage, which is shown in Fig. 8 and Table 2. Accordingly, the non-opaques make up the largest percentage of all heavy materials (61.8%), while the opaques make up 12.2. Zircon comes in second with 19.60%, followed by rutile (10.2%) and tourmaline (5.8%).

The ZTR Index values range from 64.15 to 73.08%, with an average of 68.46% (Table 2), and are calculated by dividing the total modal composition of tourmaline (T), rutile (R), and zircon (Z) by the transparent, non-micaceous, and detrital heavy minerals. According to Hubert (1962), ZTR > 75% indicates high mineralogical maturity and intense recycling, whereas 50–75% indicates moderate maturity. Thus, these sandstones are moderately mature, indicating they have undergone some degree of reworking but are not highly recycled.

**Table 1:** Summary of the mineralogical composition of Hinna Bima sandstones from the thin section study in percentage

| Sample Id | Quartz | Feldspar | Lithic Fragment |
|---|---|---|---|
| HB1 | 66 | 24 | 8 |
| HB2 | 53 | 37 | 10 |
| HB4 | 52 | 38 | 10 |
| HB5 | 38 | 52 | 10 |
| HB6 | 58 | 32 | 10 |
| HB7 | 64 | 25 | 11 |
| HB8 | 59 | 29 | 12 |
| HB9 | 52 | 37 | 11 |
| HB11 | 47 | 45 | 8 |
| HB13 | 65 | 26 | 9 |
| AVERAGE | 55.4 | 34.5 | 9.9 |

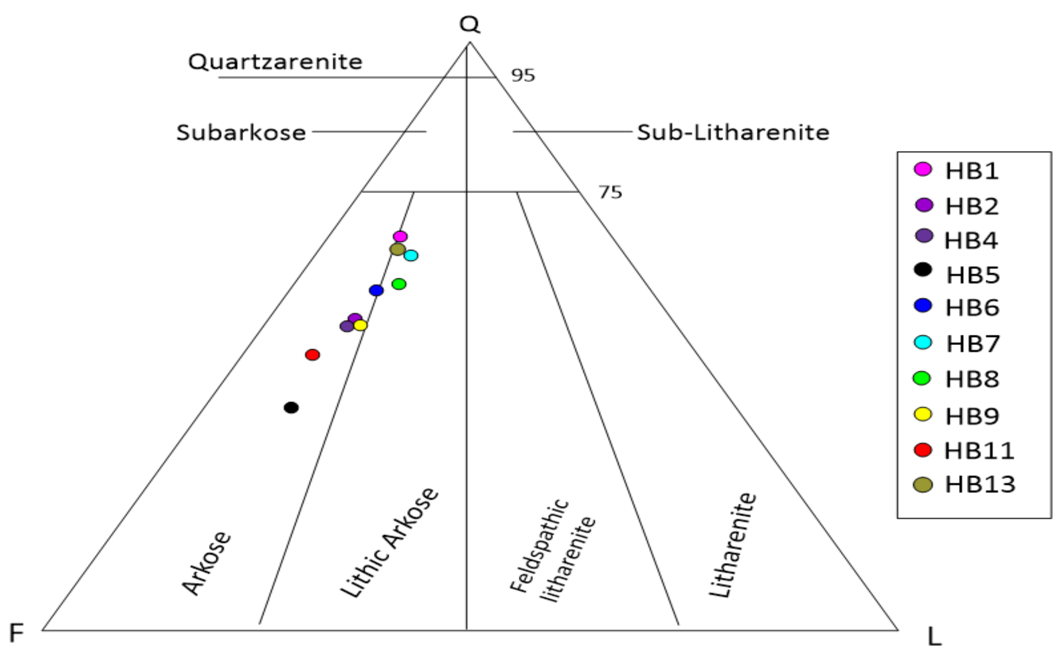


**Fig. 7:** QFL diagram depicting sandstone classification (after Folk 1980)

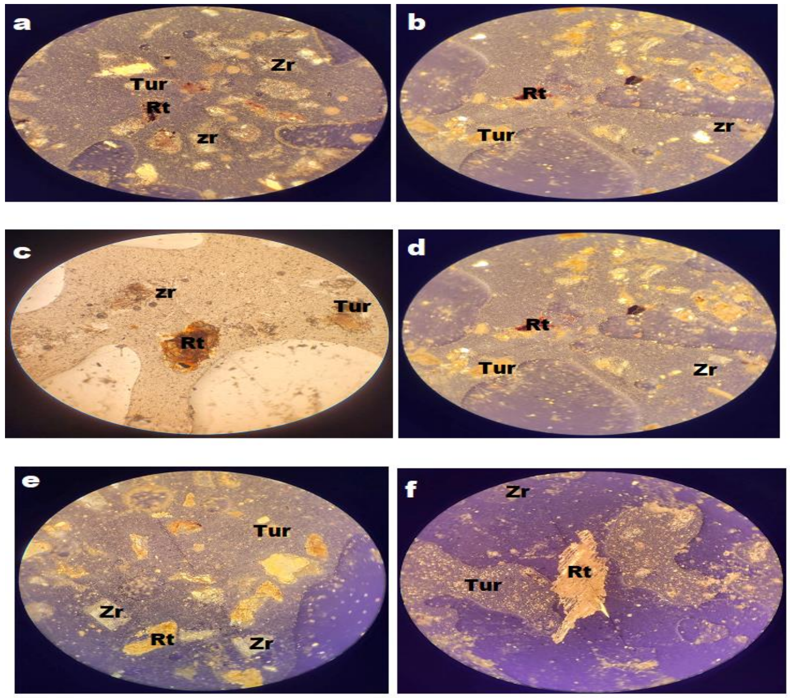


**Fig. 8:** Microphotograph showing heavy minerals in thin-sectioned sandstone (a - f), Zr = Zircon, Rt = Rutile, and Tur=Tourmaline. Mag. =X40

**Table 2:** Percentages of Zircon, Tourmaline, Rutile, and Z.T.R. index of Bima sandstones of the Hinna section

| Sample ID | Zircon | Rutile | Tourmaline | Opaque minerals | Non-Opaque mineral | ZTR INDEX |
|---|---|---|---|---|---|---|
| HB1 | 19.0 | 7.0 | 8.0 | 13.0 | 53.0 | 64.15 |
| HB5 | 23.0 | 9.0 | 5.0 | 11.0 | 52.0 | 71.15 |
| HB6 | 20.0 | 11.0 | 5.0 | 11.0 | 53.0 | 67.92 |
| HB9 | 24.0 | 10.0 | 4.0 | 9.0 | 51.0 | 73.08 |
| HB11 | 12.0 | 14.0 | 7.0 | 17.0 | 50.0 | 66.00 |
| AVERAGE | 19.60 | 10.2 | 5.8 | 12.2 | 61.8 | 68.46 |

*Major-element geochemistry*

Table 3 presents the results of geochemical analyses of the major-element concentrations in the Bima Sandstone, Hinna section. The majority of sandstone samples are rich in $SiO_2$ (61.07%–77.95%), with an average of 71.64%, making them quartz-rich according to Crook's (1974) criterion. The primary sources of silica include quartz, feldspar, and clay minerals. $Al_2O_3$ ranges in the sandstones from 14.99% to 20.56%, indicating a medium amount of feldspar and clay. The samples have lower concentrations of MgO (0.06%–0.8%), CaO (0.23%–1.65%), $K_2O$ (0.54%–2.50%), MnO (0.03%–1.25%), and $Fe_2O_3$ (1.00%–4.30%).

According to Armstrong-Altrin et al. (2004), low concentrations of $FeO_3$ and $TiO_2$ in various sandstones are usually indicative of low amounts of Ti-bearing minerals (biotite, ilmenite, and magnetite) in the samples under examination. Both MnO and $P_2O_5$ are significantly depleted, and there are no discernible differences in their concentrations in the samples. The presence of carbonate cements may be associated with the content of CaO and MgO, the abundance of iron oxide, heavy minerals, and, to a lesser extent, clay minerals containing iron, and the presence of K-feldspars (microcline and orthoclase), mica, and illite may be linked to the content of $Al_2O_3$ and $KO_3$. Plagioclase feldspar is one of the main sources of NaO. The primary sources of $TiO_2$ are rutile and Ti-opaque minerals. The existence of cement is primarily connected to the MgO content. The primary sources of CaO are the diagenesis of plagioclase and carbonate cement. Some of the key elements in Sandstone are severely diminished. This implies that ferromagnesian minerals and some feldspars were removed by extensive weathering and reworking.

**Table 3:** Major element concentrations (wt. %) of the Bima Sandstones, Hinna Section

| Oxides (%) | HB 1 | HB 2 | HB 4 | HB 5 | HB 6 | HB 7 | HB 8 | HB 9 | HB 11 | HB 13 |
|---|---|---|---|---|---|---|---|---|---|---|
| **$SiO_2$** | 74.95 | 75.97 | 77.95 | 69.31 | 64.87 | 76.65 | 64.95 | 77.61 | 73.16 | 61.07 |
| **CaO** | 0.23 | 0.30 | 0.25 | 0.40 | 1.65 | 0.76 | 1.13 | 0.70 | 0.54 | 1.33 |
| **MgO** | 0.11 | 0.09 | 0.06 | 0.12 | 0.80 | 0.23 | 0.80 | 0.22 | 0.20 | 0.70 |
| **$K_2O$** | 1.46 | 1.30 | 0.98 | 0.54 | 2.50 | 1.87 | 2.00 | 1.50 | 2.25 | 2.31 |
| **$Na_2O$** | 0.46 | 0.52 | 0.38 | 0.20 | 1.00 | 0.60 | 1.12 | 0.85 | 1.60 | 3.58 |
| **$TiO_2$** | 0.91 | 0.58 | 1.16 | 0.83 | 0.72 | 0.65 | 2.07 | 0.62 | 1.13 | 1.49 |
| **MnO** | 1.08 | 0.03 | ND | 0.54 | 1.24 | 0.03 | 0.24 | ND | 0.05 | 2.13 |
| **$P_2O_5$** | ND | ND | ND | ND | ND | ND | ND | ND | ND | ND |
| **$Fe_2O_3$** | 1.75 | 1.02 | 1.02 | 3.70 | 3.32 | 1.39 | 4.30 | 1.04 | 1.00 | 4.81 |
| **$Al_2O_3$** | 15.67 | 17.77 | 15.78 | 20.56 | 20.19 | 16.07 | 18.47 | 14.99 | 18.94 | 17.07 |
| **$H_2O^+$** | 1.65 | 1.23 | 1.10 | 3.59 | 3.68 | 1.35 | 3.40 | 1.10 | 1.85 | 4.50 |
| **CIA** | 85.05 | 86.35 | 88.06 | 86.82 | 75.10 | 75.38 | 76.68 | 75.48 | 81.83 | 61.23 |
| **PIA** | 92.30 | 92.11 | 93.17 | 88.73 | 81.43 | 81.33 | 82.52 | 80.46 | 89.84 | 63.69 |
| **CIW** | 93.02 | 92.69 | 93.60 | 89.02 | 83.51 | 83.29 | 84.25 | 82.20 | 90.97 | 67.26 |
| **ICV** | 0.44 | 0.25 | 0.33 | 0.41 | 0.58 | 0.49 | 0.71 | 0.48 | 0.37 | 1.10 |
| **$Al_2O_3/SiO_2$** | 0.20 | 0.23 | 0.20 | 0.30 | 0.31 | 0.21 | 0.28 | 0.19 | 0.26 | 0.28 |
| **$K_2O/Na_2O$** | 3.17 | 2.50 | 2.58 | 2.70 | 2.50 | 3.12 | 1.80 | 1.80 | 1.41 | 0.65 |
| **$Al_2O_3/TiO_2$** | 17.22 | 30.64 | 13.60 | 24.77 | 28.04 | 24.72 | 8.92 | 24.18 | 16.76 | 11.46 |
| **DF 1** | -3.21 | -5.02 | -3.90 | -4.93 | -2.03 | -3.07 | -3.40 | -2.82 | -3.60 | -2.86 |
| **DF 2** | -2.88 | -3.83 | -1.55 | -1.65 | -1.08 | -4.11 | -2.47 | -0.11 | -3.64 | -0.40 |

ND = not detected; $Fe_2O_3$ is the expression for total Fe. CIA is equal to. CIA = $[Al_2O_3/ (Al_2O_3 + CaO^* + Na_2O + K_2O)] \times 100$; PIA = $[(Al_2O_3 - K_2O)/ (Al_2O_3 + CaO^* + Na_2O + K_2O)] \times 100$. (Nesbitt 2 and Young, 1982) CIW = $[Al_2O_3\ 3/ (Al_2O_3 + CaO^* + Na_2O)] \times 100$ ICV = $(Fe_2O_3 + K_2O + Na_2O + CaO + MgO + MnO + TiO_2)/Al_2O_3$ (Cox et al., 1995)

*Geochemical classification*

From the geochemical classification of Pettijohn et al (1972), based on the values of Log ($Na_2O/K_2O$) versus Log ($SiO_2/Al_2O_3$), the sample were mostly plotted into arkose and lithic arkose with only one sample in the graywacke sandstone field (Fig. 9a). While from the geochemical classification based on the relative proportions of $Fe_2O_3$ + MgO, $Na_2O$, and $K_2O$, reveals that most of the samples are distributed across the arkose field except two samples which falls within the lithic sandstone and graywacke fields (Pettijohn et al, 1987; Fig. 9b), this geochemical classification is which is consistent with the Folk classification scheme (Fig. 7).

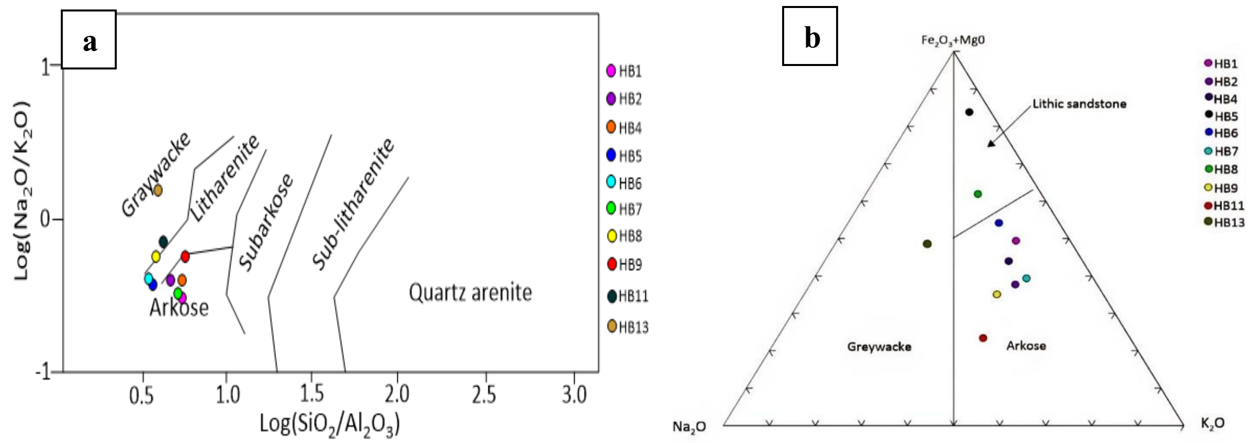


**Fig. 9:** Chemical classification of the Sandstone based on (a) the log ($SiO_2$ /$Al_2O_3$) vs. log ($Na_2O$/$K_2O$) diagram of Pettijohn et al. (1972) and (b) Ternary plot of $Fe_2O_3$ + MgO - $Na_2O$ - $K_2O$ (after Pettijohn et al., 1987).

*Facies Associations and Depositional Environment*

The vertical and lateral arrangement of the identified lithofacies allows their grouping into three genetically related facies associations: (i) proximal braided river, (ii) braided river in-channel, and (iii) floodplain/overbank.

*Facies Association I: Proximal Braided River*

The proximal braided river association (Gtt and Gtb facies) is dominated by coarse- to very coarse-grained, gravelly sandstones with erosional basal contacts, poor sorting, and abundant pebble and mud-clast lags. Thick, amalgamated channel bodies and the prevalence of trough and planar cross-bedding indicate deposition under high-energy, unidirectional flow conditions. The coarse-grain size, textural immaturity, and abundance of basement-derived clasts suggest short transport distances and rapid sediment delivery from uplifted source areas, typical of syn-rift settings proximal to active fault margins.

*Facies Association II: Braided River in-channel*

The braided river in-channel association (St, Sp, and Sm facies) consists mainly of medium- to coarse-grained sandstones with well-developed trough and planar cross-bedding, locally massive units, and laterally extensive channel bodies. Fining-upward trends from erosional bases into better-sorted tops reflect bar migration and channel-fill processes within active braided river systems. This association represents a slightly more distal yet still high-energy fluvial environment and corresponds to the main aggradational phase of braided-channel development within the basin.

*Facies Association III: Floodplain/Overbank*

This association consists of Fm, F11, and F12 facies. The floodplain/overbank association is characterized by finer-grained sandstones, siltstones, and mudstones, commonly showing planar lamination and massive bedding. These facies reflect deposition from waning flood flows and suspension settling on floodplains adjacent to active channels. Their stratigraphic position above channelized facies indicates a progressive reduction in depositional energy, likely linked to basin filling and lateral migration of channel belts rather than complete tectonic quiescence. The facies architecture and stacking patterns indicate deposition in a braided fluvial system within a fault-controlled continental rift basin. The transition from gravel-dominated proximal facies to sand-dominated channel and floodplain deposits records internal basin reorganization during continued syn-rift sedimentation.

*Paleoenvironment*

The sedimentary architecture and facies stacking patterns of the Middle Bima Member at Hinna reflect deposition within a continental braided fluvial system expressed through three recurring facies associations. The lower to middle parts of the succession are dominated by the proximal braided river facies association, characterized by gravelly and coarse-grained sandstones with erosional basal contacts and amalgamated channel bodies, indicating high-energy channel environments and substantial bedload transport. These pass upward into the braided river in-channel facies association, composed mainly of trough- and planar-cross-bedded sandstones representing migrating bars and dunes within active channel belts.

Toward the upper part of the section, the increasing occurrence of the floodplain and overbank facies association, consisting of fine-grained siltstone and mudstone with subordinate fine sandstones, reflects reduced flow energy, channel abandonment, and enhanced suspension settling during waning flood stages. The vertical transition from channel-dominated to floodplain-dominated facies indicates progressive development of low-energy depositional environments within an overall braided fluvial system.

*Tectonic setting*

More recent multidimensional discrimination functions (Verma & Armstrong-Altrin, 2013), which are better suited for distinguishing tectonic settings, consistently place the Bima Sandstone samples within the continental rift field (Fig. 10). This interpretation is further supported by petrographic evidence of arkosic to lithic arkosic compositions, abundant feldspar, and basement-derived lithic fragments, indicating short transport distances and rapid sediment supply from nearby Precambrian source areas. The enrichment in $SiO_2$ and the depletion in $Fe_2O_3$, MgO, and CaO are consistent with felsic source rocks in continental crustal settings.

Plotting of detrital modes (Q-F-L) of the studied sandstones on the diagrams of Dickinson et al. (1983) indicates that the tectonic provenance of the studied sandstones was plotted in the recycled orogenic fields, while some of the samples fall within the basement uplift field (Fig. 11). This shows that they were sourced from uplifted and eroded older sedimentary or metasedimentary rocks. The high quartz content indicates textural maturity, a product of cyclic sediment reworking, consistent with the tectonic models for the Benue Trough.

The regional geological evolution of the Gongola Basin corroborates a rift-related setting. The basin developed as part of the West and Central African Rift System in response to extensional tectonics associated with the opening of the South Atlantic. Normal faulting produced horst-and-graben architectures and uplifted basement blocks that served as the principal sediment sources for the Bima Sandstone, exerting strong control on accommodation creation and sediment dispersal. The Bima Sandstone is therefore best interpreted as a syn-rift siliciclastic succession deposited within an intracontinental rift basin influenced by inherited felsic crustal composition.

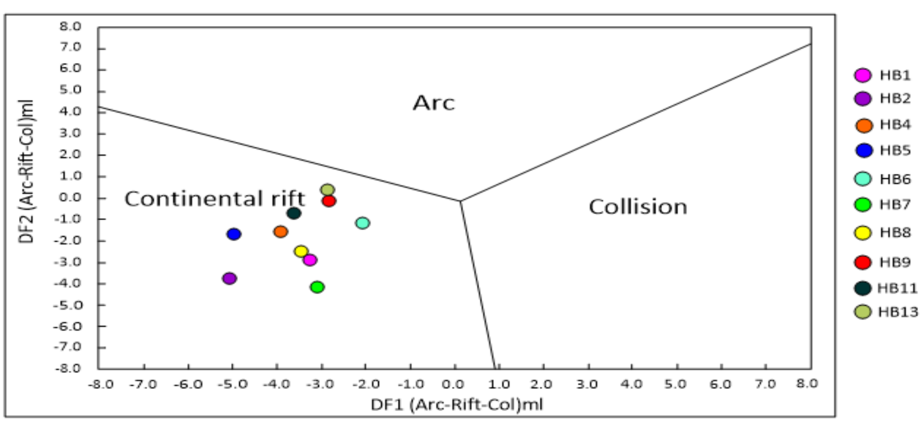

**Fig. 10:** Tectonic Discriminant-function diagram for high-silica clastic sediments from 3 tectonic settings, after (Verma & Armstrong-Altrin, 2013)

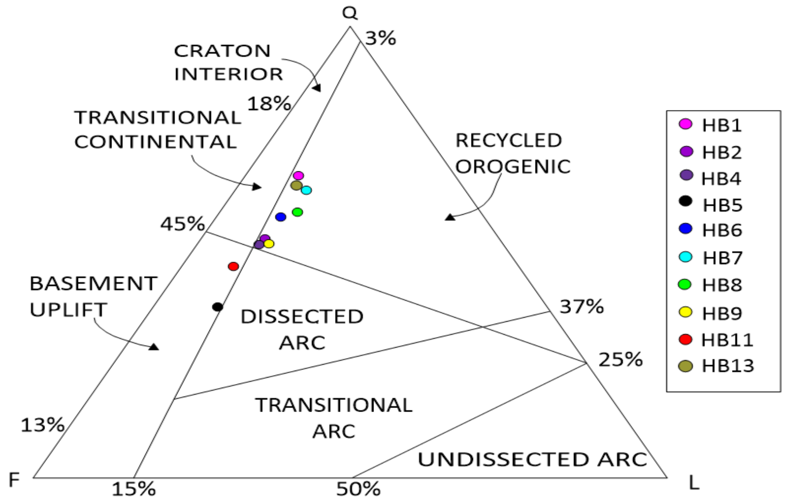


**Fig. 11:** QFL ternary diagrams of tectonic/provenance for the Bima Sandstone (Dickson et al., 1983))

*Provenance*

Provenance analysis of the Bima Sandstone integrates petrographic, geochemical, and heavy-mineral data to reconstruct the nature of its source rocks. Modal composition reveals quartz-dominated sandstones (40-66%) with subordinate feldspar (20-45%) and lithic fragments (8.0-14%). The high proportion of monocrystalline quartz, coupled with K-feldspar, reflects derivation from stable continental crust, particularly granitic and gneissic terranes. The presence of sedimentary lithic fragments also reflects contributions from older sedimentary successions that were recycled during deposition.

The high zircon contents indicate derivation from felsic igneous rocks (granites, rhyolites). Medium rutile content indicates metamorphic/high-T contributions (gneisses, granulites, schists). Rutile is common as an accessory in medium- to high-grade metamorphic rocks and some igneous rocks. The higher rutile in (HB11) reflects a metamorphic component in the source mix. These heavy-mineral percentages reflect a predominantly felsic continental/recycled-sediment source with a metamorphic contribution and minor mafic input, deposited under conditions of moderate mineralogical maturity. The sandstones are not compositionally ultra-mature (since ZTR < 75%). This indicates moderate chemical weathering and transport, probably under fluvial–deltaic systems with limited recycling, consistent with derivation from nearby basement uplifts within a continental block to a recycled orogen setting of the Benue Trough.

The concentrations of major and trace elements in siliciclastic sedimentary rocks have been used to determine their provenance. This is because certain oxides (e.g., $Al_2O_3$ and $TiO_2$) and trace elements exhibit low mobility during transport, weathering, and diagenesis of host rocks (Augustsson et al., 2023; Hayashi et al., 1997). Intermediate igneous source rocks contain $Al_2O_3/TiO_2$ ratios ranging from 8 to 21, while mafic igneous source rocks have ratios between 3 and 8. So, $Al_2O_3/TiO_2$ ratios between 21 and 70 also imply felsic igneous source rocks. The examined sandstones have $Al_2O_3/TiO_2$ ratios ranging from 9.0 to 30.6. These ratios are comparable to those of felsic and intermediate igneous provenance (Hayashi et al., 1997). The sandstones are enriched in $SiO_2$ but depleted in $Fe_2O_3$, MgO, CaO, and $TiO_2$, characteristics typical of felsic rather than mafic source rocks.

The above observation indicates that the Bima Sandstone was derived primarily from Precambrian basement complexes comprising granitic, gneissic, and metamorphic rocks, with additional contributions from recycled sedimentary successions. This provenance pattern reflects the tectonic evolution of the Gongola Basin, where rifting and faulting during the Early Cretaceous exposed basement terranes that supplied sediments to the developing fluvial systems. Thus, the Bima Sandstone represents a multi-source assemblage recording both first-cycle and recycled inputs in a continental rift setting.

*Paleoweathering*

Paleoweathering conditions of the Bima Sandstone were assessed using geochemical indices and mineralogical data, which together provide insight into the intensity of chemical weathering in the source region. Mineralogically, the depletion of ferromagnesian minerals (such as olivine and pyroxene), the low abundance of albite (plagioclase feldspar) and microcline (K-feldspar), and the percentage of monocrystalline quartz grains relative to polycrystalline ones indicate that the source rocks have undergone significant chemical weathering (Wanas & Assal, 2021).

The A–CN–K ternary diagram shows weathering trends parallel to the predicted line of Nesbitt and Young (Fig. 11a), indicating progressive depletion of Ca and Na relative to Al during chemical weathering of felsic source rocks. These trends are consistent with petrographic evidence of feldspar alteration and support a humid-to-semi-humid paleoclimate during sediment generation. Major-element geochemistry and weathering indices provide additional constraints on paleoweathering conditions in the source area. Elevated CIA, CIW, and PIA (Table 3) values indicate moderate to intense chemical weathering of feldspar-rich source rocks, leading to the breakdown of plagioclase and K-feldspar and the formation of clay minerals. This intense chemical weathering was also confirmed by the binary diagram of McLennan et al. (1993) (Fig. 11b). Most samples display ICV values <1, consistent with advanced chemical weathering and compositional maturity. However, one sample with lower CIA values likely reflects localized sediment mixing or reduced weathering intensity. The paleoweathering signatures of the Bima Sandstone reflect erosion of felsic basement terranes subjected to moderate to intense chemical weathering, followed by short-distance transport and deposition within a syn-rift braided fluvial system.

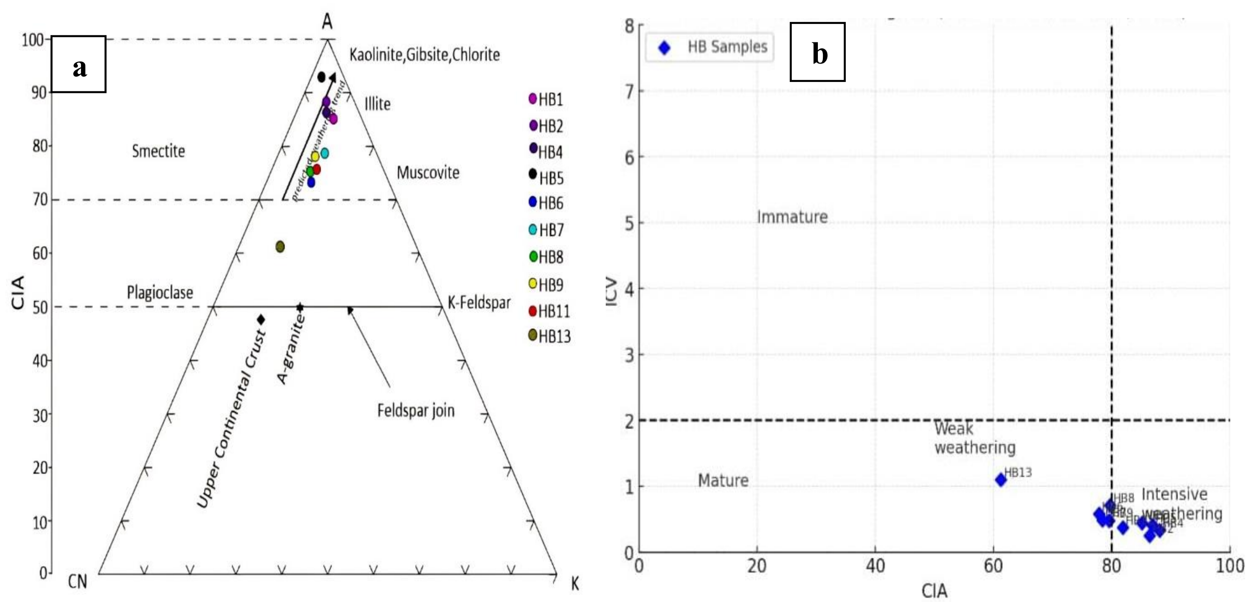


**Fig. 11:** (a) The A-CN-K ternary plot of the sandstone samples; A, $Al_2O_3$; CN, CaO* $+Na_2O$; K, $K_2O$; CIA*, Chemical Index of Alteration (after Nesbitt and Young 1982). (b) The binary diagram of CIA versus ICV after McLennan et al. (1993)

**CONCLUSION**

The sedimentological and geochemical data demonstrate that the Bima Sandstone at Hinna was deposited within a fault-controlled continental rift basin during Early Cretaceous extension in the Gongola Basin. Facies stacking patterns defined by proximal braided river, in-channel braided river, and floodplain/overbank associations indicate deposition in a high-energy braided fluvial system that evolved toward lower-energy conditions as the basin filled. Petrographic compositions and heavy mineral assemblages dominated by quartz, feldspar, zircon, rutile, and tourmaline indicate derivation mainly from felsic igneous and high-grade metamorphic rocks of the Nigerian Basement Complex, with minor recycled sedimentary input. Geochemical proxies and weathering indices reveal moderate to intense chemical weathering of source terranes prior to deposition. Tectonic discrimination diagrams consistently support a continental rift setting, reflecting syn-rift uplift, short transport distances, and rapid sediment supply from adjacent basement highs. The Bima Sandstone, therefore, represents a multi-cycle, syn-rift braided fluvial succession that records the early tectono-sedimentary evolution of the Northern Benue Trough. These findings provide a robust framework for regional correlation, paleogeographic reconstruction, and improved understanding of reservoir distribution within rift-related continental basins.

**Acknowledgement**
The authors sincerely acknowledge the Department of Geology, Bayero University, Kano, for providing access to field equipment and the petrographic laboratory facilities used in this research. Gratitude is also extended to colleagues and field assistants whose contributions during sampling and data collection were invaluable. This study benefited from the guidance and encouragement of academic mentors within the department. Their contributions were invaluable to the successful completion of this research.

**Funding**
No funding was received to assist with the preparation of this manuscript.

**Author contributions**
Ahmad Umar Ibrahim Bebi designed the study while Sani Kasim supervised, reviewed, and edited the manuscript.

**Availability of Data/Materials**
The data that support the findings of this study are available on request from the corresponding author.

**REFERENCES**

Abubakar, M. B. (2006). Biostratigraphy, paleoenvironment, and organic geochemistry of the Cretaceous sequences of the Gongola Basin, Upper Benue Trough, Nigeria (Unpublished PhD thesis). Abubakar Tafawa Balewa University, Bauchi, Nigeria.

Abubakar, M. B., Dike, E. F. C., Obaje, N. G., Wehner, H., & Jauro, A. (2008). Petroleum prospectivity of Cretaceous formations in the Gongola Basin, Upper Benue Trough, Nigeria: An organic geochemical perspective on a migrated oil controversy. *Journal of Petroleum Geology, 31*(4), 387–408.

Augustsson, C., Aehnelt, M., Olivarius, M., Voigt, T., Gaupp, H., & Hilse, U. (2023). Provenance from the geochemical composition of terrestrial clastic deposits: A review with a case study from the intracontinental Permo-Triassic of European Pangea. *Sedimentary Geology, 456,* Article 106496. https://doi.org/10.1016/j.sedgeo.2023.106496

Benkhelil, J. (1982a). Benue Trough and Benue Chain. *Geological Magazine, 119*, 153–155. https://doi.org/10.1017/S001675680002584X

Benkhelil, J. (1982b). The structural map of the Upper Benue Valley. *Nigerian Journal of Mining and Geology, 18,* 140–145.

Benkhelil, J. (1989). The origin and evolution of the Cretaceous Benue Trough, Nigeria. *Journal of African Earth Sciences, 8,* 251–282.

Benkhelil, M. J. (1983). Is the Benue Trough a ridge? *Bulletin du Centre de Recherches Exploration-Production Elf-Aquitaine, 7,* 315–321.

Bhatia, M. R. (1983). Plate tectonics and geochemical composition of sandstones. *Journal of Geology, 91,* 611–624. https://doi.org/10.1086/628815

Bhatia, M. R. (1985). Rare earth element geochemistry of Australian Paleozoic greywackes and mudrocks: Provenance and tectonic control. *Sedimentary Geology,* 45, 97–113.

Bhatia, M. R., & Crook, K. W. (1986). Trace element characteristics of greywackes and tectonic setting discrimination of sedimentary basins. *Contributions to Mineralogy and Petrology, 92,* 181–193.

Burke, K. G. A., & Dewey, J. F. (1973). Plume-generated triple junctions. *Journal of Geology, 86,* 406–433. https://doi.org/10.1086/627882

Cox, R., Lowe, D. R., & Cullers, R. L. (1995). The influence of sediment recycling and basement composition on the evolution of mudrock chemistry in the southwestern United States. *Geochimica et Cosmochimica Acta, 59,* 2919–2940.

Critelli, S., Arribas, J., Le Pera, E., Tortosa, A., Marsaglia, K. M., & Latter, K. K. (2003). The recycled orogenic sand provenance is from an uplifted thrust belt in the Betic Cordillera, southern Spain. *Journal of Sedimentary Research, 73,* 72–81. https://doi.org/10.1306/071002730072

Dickinson, W. R. (1985). Interpreting provenance relations from detrital modes of sandstones. *In Provenance of Arenites* (pp. 333–361). Springer.

Dickinson, W. R. (1988). Provenance and sediment dispersal in relation to paleotectonics and paleogeography of sedimentary basins. *In New Perspectives in Basin Analysis* (pp. 3–25). Springer.

Dickinson, W. R., & Suczek, C. A. (1979). Plate tectonics and sandstone compositions. *American Association of Petroleum Geologists Bulletin, 63,* 2164–2182.

Fairhead, J.D., Green, C.M., Masterton, S.M. & Guiraud, R. (2013). The roles of plate tectonics, inferred stress changes, and stratigraphic unconformities in the evolution of the West and Central African Rift System and the Atlantic continental margins. *Tectonophysics, 594, 118–127.*

Falconer, J. D. (1911). *The geology and geography of northern Nigeria* (p. 295). Macmillan.

Folk, R. L., & Ward, W. C. (1957). A study of the significance of grain-size parameters. *Journal of Sedimentary Petrology, 27,* 3–26. https://doi.org/10.1306/74d70646-2b21-11d7-8648000102c1865d

Gaillardet, J., Dupré, B., & Allègre, C. (1999). Geochemistry of large river suspended sediments: Silicate weathering or recycling tracer? *Geochimica et Cosmochimica Acta, 63,* 4037–4051. https://doi.org/10.1016/S0016-7037(99)00307-5

Garzanti, E., & Andò, S. (2007). Heavy mineral concentration in modern sands: Implications for provenance interpretation. In M. A. Mange & D. T. Wright (Eds.), *Heavy Minerals in Use* (Vol. 1283). Elsevier.

Grant, N. K. (1971). The South Atlantic, Benue Trough, and Gulf of Guinea Cretaceous triple junction. *Bulletin of the Geological Society of America, 82,* 2295–2298.

Guiraud, M. (1990). Tectono-sedimentary framework of the Early Cretaceous continental Bima Formation (Upper Benue Trough), NE Nigeria. *Journal of African Earth Sciences, 10,* 341–355.

Harnois, L. (1988). The CIW index: A new chemical index of weathering. *Sedimentary Geology, 55,* 319–322.

Hayashi, K., Fujisawa, H., Holland, H., & Ohmoto, H. (1997). Geochemistry of ~1.9 Ga sedimentary rocks from northeastern Labrador, Canada. *Geochimica et Cosmochimica Acta, 61,* 4115–4137.

Hubert, J. F. (1962). A zircon–tourmaline–rutile maturity index and the interdependence of the composition of heavy mineral assemblages with the gross composition and texture of sandstones. *Journal of Sedimentary Petrology*, **32**, 440–450.

Ingersoll, R. V., Bullard, T., Ford, R., Grimm, J., Pickle, J., & Sares, S. (1984). The effect of grain size on detrital modes: A test of the Gazzi–Dickinson point-counting method. *Journal of Sedimentary Research, 54,* 103–116.

King, I. C. (1950). Speculation on the outline and the mode of disruption of Gondwanaland. *Geological Magazine, 87,* 353–359.

Kroonenberg, S. B. (1994). Effects of provenance, sorting, and weathering on the geochemistry of fluvial sands from different tectonic and climatic environments. *Proceedings of the 29th International Geological Congress, Part A,* 69–81.

McLennan, S. M., Hemming, S., McDaniel, D. K., & Hanson, G. N. (1993). Geochemical approaches to sedimentation, provenance, and tectonics. In M. J. Johnsson & A. Basu (Eds.), *Processes Controlling the Composition of Clastic Sediments* (Special Paper 284, pp. 21–40). Geological Society of America. https://doi.org/10.1130/SPE284-p21

Miall, A. D. (1996). *The geology of fluvial deposits: Sedimentary facies, basin analysis and petroleum geology.* Springer.

Miall, A. D. (2000). *Principles of sedimentary basin analysis* (3rd ed.). Springer.
Miall, A.D. (2006). *The geology of fluvial deposits (4th ed.): Springer-Verlag, Berlin, 191 p*.
Miall, A.D. (2010). Alluvial deposits. In: James, N.P., Dalrymple, R.W. (eds) Facies models 4, *Geological Association of Canada, St. John's, Newfoundland, GEO text 6, pp 105–137*
Miall, A.D. (2014). Fluvial Depositional Systems. *Springer Int. Pub., Switzerland, 43p.*

Morton, A. C., & Hallsworth, C. (1994). Identifying provenance-specific features of detrital heavy mineral assemblages in sandstones. *Sedimentary Geology, 90,* 241–256.

Nesbitt, H. W., & Young, G. M. (1984). Prediction of some weathering trends of plutonic and volcanic rocks based on thermodynamic and kinetic considerations. *Geochimica et Cosmochimica Acta, 48,* 1523–1534.

Nichols, G. J. (2009). *Sedimentology and Stratigraphy*. John Wiley and Sons, New York, *p. 452*

Nwajide, C. S. (2013). *Geology of Nigeria sedimentary basins* (*p. 565*). CSS Bookshops Ltd.

Obaje, N. G., Wehner, H., Abubakar, M. B., & Isah, M. T. (2004). Nasara 1 well, Gongola Basin (Upper Benue Trough, Nigeria): Source rock evaluation. *Journal of Petroleum Geology, 27*(2), 191–206.

Petters, S. W. (1978). Stratigraphic evolution of the Benue Trough and its implication for the Upper Cretaceous paleogeography of West Africa. *Journal of Mining and Geology, 86,* 311–321.

Pettijohn, F. J., Potter, P. E., & Siever, R. (1987). *Sand and sandstones* (2nd ed.). Springer.

Roser, B. P., & Korsch, R. J. (1986). Determination of tectonic setting of sandstone–mudstone suites using $SiO_2$ content and $K_2O$ ratio. *Journal of Geology, 94,* 635–650.

Roser, B. P., & Korsch, R. J. (1988). Provenance signatures of sandstone–mudstone suites were determined using discriminant function analysis of major-element data. *Chemical Geology, 67,* 119–139. https://doi.org/10.1016/0009-2541(88)90010-1

Samaila, N. K., Obaje, N. G., & Dada, S. S. (2001). Geochemical classification of Cretaceous Bima Sandstone from the Gongola Arm, Upper Benue Trough, N.E. Nigeria. *Science Forum Journal of Pure and Applied Science, 4*(2), 190–197.

Shettima, B., Dike, E. F. C., Abubakar, M. B., & Muhammad, A. V. (2007). Facies and facies architecture of the Cretaceous Yolde Formation in the Gongola Basin, Upper Benue Trough, Nigeria. *NMGS 43rd Annual International Conference Abstracts, 48,* 123–137.

Sarki Yandoka, B. M., Abubakar, M. B., Abdullah, W. H., Amir Hassan, M. H., Bappah, U. A., John, S. J., & Abdulkarim, H. A. (2014). Facies analysis, paleoenvironmental reconstruction, and stratigraphy of the Early Cretaceous sediments (Lower Bima

Member) in the Yola Sub-basin, Northern Benue Trough, NE Nigeria. *Journal of African Earth Sciences, 96,* 168–179.

Sarki Yandoka, B. M., Abubakar, M. B., Abdullah, W. H., Maigari, A. S., & Muhammed, H. H. (2015). Sedimentology, geochemistry, and paleoenvironmental reconstruction of the Cretaceous Yolde Formation from Yola Sub-basin, Northern Benue Trough, NE Nigeria. *Marine and Petroleum Geology, 67,* 663–677.

Tukur, A., Samaila, N.K., Grimes, S.T., Kariya, I.I., & Chaanda, M.S. (2015). Two-member subdivision of the Bima Sandstone, Upper Benue Trough, Nigeria: Based on sedimentological data. *Journal of African Earth Sciences 104, 140–158.*

Verma, S. P., & Armstrong-Altrin, J. S. (2013). New multi-dimensional diagrams for tectonic discrimination of siliciclastic sediments and their application to Precambrian basins. *Chemical Geology, 355,* 117–133.

Wanas, H. A., & Assal, E. M. (2021). Provenance, tectonic setting, and source area paleoweathering of sandstones of the Bahariya Formation, Bahariya Oasis, Egypt. *Sedimentary Geology, 413,* 105822. https://doi.org/10.1016/j.sedgeo.2020.105822

Wright, J. B. (1968). Review of the origin and evolution of the Benue Trough in Nigeria. *Journal of African Earth Sciences, 2,* 10–98.

Zaborski, P. M., et al. (1997). Stratigraphy and structure of the Cretaceous Gongola Basin, northeastern Nigeria. *Bulletin du Centre de Recherches Exploration-Production Elf Aquitaine, 21*(1), 153–185.

Zaborski, P. M. (2003). Guide to the Cretaceous System in the upper part of the Upper Benue Trough, NE Nigeria. *African Geoscience Review, 10*(1–2), 13–32